

The baryonic self similarity of dark matter.

Alard, C.

Institut d'Astrophysique de Paris, 98bis boulevard Arago, 75014 Paris, France

alard@iap.fr

Received _____; accepted _____

ABSTRACT

The cosmological simulations indicates that the dark matter haloes have specific self similar properties. However the halo similarity is affected by the baryonic feedback. By using the momentum driven winds as a model to represent the baryon feedback, an equilibrium condition is derived which directly implies the emergence of a new type of similarity. The new self similar solution has constant acceleration at a reference radius for both dark matter and baryons. This model receives strong support from the observations of galaxies. The new self similar properties implies that the total acceleration at larger distances is scale free, the transition between the dark matter and baryons dominated regime occurs at a constant acceleration, and the maximum amplitude of the velocity curve at larger distances is proportional to $M^{\frac{1}{4}}$. These results demonstrate that this self similar model is consistent with the basics of MOND phenomenology. In agreement with the observations the coincidence between the self similar model and MOND breaks at the scale of clusters of galaxies. Some numerical experiments show that the behavior of the density near the origin is closely approximated by a Einasto profile.

Subject headings: cosmology: dark matter — galaxies: kinematics and dynamics

1. Introduction.

The numerical simulations of structure formation in the cosmological context has been providing us with a large wealth of interesting information about the structure of cold dark matter (CDM) haloes. Among the results from the numerical simulations two remarkable facts stands out, an universal dark matter profile (Navarro, Frenk, & White (1997), Navarro et al. (2010)), and the occurrence of a power law behavior for the pseudo phase space density, Taylor, & Navarro (2001), Ludlow et al. (2010). As an example Ludlow et al (2010) demonstrated that the residual to the fit of a power law to the pseudo phase space density $Q(r) = \frac{\rho}{\sigma^3}$ is typically about 10 to 20 % and does not exceed 30 %. This behavior is observed in a range of about 2 decades. Similar results were also derived by Navarro et al. (2010) using Aquarius data. The power law regime for $Q(r)$ has a well defined outer boundary, while the inner regime is more difficult to probe due to the intrinsic difficulty of reconstructing the complex evolution of the phase space density when the system experiences a large number of multi-dimensional folds in phase space. The agreement between the power law exponent and the prediction from the Bertschinger self similar solution (Bertschinger (1985)) suggested that the CDM haloes had self similar properties. However the Bertschinger solution is a purely radial solution which does not corresponds to the haloes obtained in numerical simulations. The reason for the correct prediction of $Q(r)$ exponent is due to the fact that Bertschinger’s solution belongs to a family of self similar solutions with the same specific values of the constants. The actual solution belongs to the same family but with completely different density and velocity dispersion, only the pseudo phase space density and other related quantities are the same in this family of solutions (Alard (2013)). Thus Bertschinger’s solution should be seen in historical perspective as the first clue to suggest the self similar nature of the real solution. A puzzling unsolved problem was the reason for the observed power law behavior of the pseudo phase space density, and the non power law behavior of other quantities. Alard

(2013) demonstrated that dynamically cold self similar solutions in a quasi equilibrium situation have pseudo phase space density with power law behavior. This result derive from the fact that the smoothed probability distribution $P(f)$ of f remains self similar (Alard 2013). A direct prediction is that the higher order moments constructed using $P(f)$ should also be power laws with predictable exponents. These predicted power laws are effectively consistent with the measurements obtained using data from numerical simulations (Alard 2013). Other quantities like the smoothed density do not have a self similar expectation, and thus are not power laws near equilibrium. At this point it is important to note that these results obtained with an intrinsically cold dark matter model are incompatible with self similar models developed in the fluid limit (see for instance Subramanian (2000) or Lapi & Cavaliere (2011)). The cold model is not analog to a continuous model, this fundamental difference is related to the different behavior of $Q(r)$ and other related quantities, and non self similar smoothed quantities like $\rho(r)$ or $\sigma(r)$. Thus $Q(r)$ and higher order moments of the probability distribution of f are fundamental and specific in the cold non fluid approach only. As a consequence the consistency between self similarity and the near equilibrium phase space density corresponding to the collapse of dynamically cold initial fluctuation is well established. This description of pure CDM halos has to be modified to take into account the baryon population co-existing with the DM in real galaxies. The baryonic feedback modifies the mass distribution and as a result influences the DM halo through changes in the gravitational potential. This mechanism leads to a much more complex picture. A good illustration of this picture is given by the recent observations of the rotation curves of galaxies, and in particular from the THINGS survey (Walter et al. (2008)) The high quality rotation curves from De Blok et al. (2008), Oh et al. (2011a) show that the central density core slope is lower than the expectation from the NFW profile. These strong and indisputable discrepancies between the observations and the expectation from the CDM model have always been a serious problem for the cold dark

matter approach. Two different type of solution have been proposed to solve this issue, first CDM is not valid and must be replaced by another model, like for instance MOND Milgrom (1983), Milgrom (1986). Interestingly Gentile et al. (2011) show that the THINGS survey rotation curves are consistent with MOND. The second solution is to consider that the baryonic feedback is sufficient to produce the softening of the DM density cusp, and this is the solution that will be considered here . The baryonic feedback has a particularly strong effect on the central region of the DM halo by flattening the initial density cusp. Using hydro dynamical simulations Oh et al. (2011b) show that the baryonic feedback model is consistent with the THINGS survey data. Since the baryons are coupled to the DM through gravitational interaction, the destruction of the central DM cusp is produced through rapid fluctuations of the gravitational potential due to the ejection of gas and dust. This cusp smoothing mechanism has been investigated in details by, Navarro, Eke, & Frenk (1996), Read, & Gilmore (2005), Pontzen & Governato (2012), Teyssier et al. (2013) who demonstrated that this mechanism is efficient and offers a possibility to reconcile CDM and the observations. The process operates through a cycle of gas ejection and re-accretion, however it is interesting to note that the re-accretion of the gas does not produce a compensation of the effects on the DM core Pontzen & Governato (2012). See Pontzen & Governato (2014) for a general review on the baryonic feedback model. Note that the observations and the numerical simulations both suggests that central density core is not completely flat. The problem of the asymptotic slope at the origin of the central core has been studied by, Oh et al. (2011a), Pontzen & Governato (2013), Di Cintio et al. (2013). Imposing a baryonic scale length to the dark matter halo indicates that the scaling relations are affected by the baryons in a way that may not be compatible with the initial similarity class and could result in the development new type of baryonic induced similarity. This model is supported by the results from high resolution hydro-dynamical simulations, where the baryonic feedback influence the DM halo parameters and in particular the

pseudo phase space density, Butsky & Maccio (2014). The idea of an universal similarity class for the rotation curve of galaxies was already introduced by Persic, Salucci, & Stel (1996), Salucci, & Persic (1997), Salucci et al. (2007), Donato et al. (2009). As we shall see this new similarity class has also some relation to the MOND phenomenology and provide an explanation to the scale independent accelerations observed at a typical radius for a large number of galaxies (Gentile et al. (2009)). Note that in the continuation we distinguish between 'scale independence' and 'self similarity'. In the forthcoming sections scale independence will mean independent of the distance scale (basically the size of the galaxy), while self similarity will mean independent on the scale of all the variables (distance, velocity, time, see Alard (2013) Section 3).

2. The baryonic scaling.

There is an extensive literature on the baryonic feedback model already existing. As an example (Navarro, Eke, & Frenk (1996), Gnedin & Zhao (2002), Read, & Gilmore (2005), Ragone-Figueroa, Granato, & Abadi (2012), Ogiya, & Mori (2012)) developed various models and investigations to document the effect of the baryonic feedback on the central parts of the DM halos. These works use the effects of supernovae and AGN to drive the baryonic feedback. The effect of supernovae tends to be dominant for low mass galaxies (see Governato et al. (2012) for more details), however there are several mechanisms involved in the supernovae feedback. The supernovae outflow may be driven through "bursty energy transfer" Governato et al. (2012), or through momentum driven wind Murray, Quataert & Thompson (2005), Oppenheimer, & Davé (2006), Davé et al. (2007), Oppenheimer & Davé (2008). The model presented here will consider the momentum driven winds as the source of baryonic feedback. Interestingly, Oppenheimer, & Davé (2006) found that among 12 others models tested the momentum driven outflow model

adjusted on local starburst data was the only one to reproduce the inter galactic medium enrichment data. In the momentum driven wind model the radiation from young stars impinges on dust in the outflow, which then couples to the gas and propels matter out of the galaxy. The associated outflow of baryonic matter affects the kinematics of the dark halo, with a dominant effect in the central area. This baryonic feedback leads to the suppression of the central density cusp and its replacement with a nearly constant or lower density slope central core. As a consequence the scale length of the dark matter halo r_{DM} is imposed by the baryonic processes, and should be closely related to the baryonic distribution size r_B . The foundations of this model are directly derived from the observational analysis of the rotation curves of galaxies. A correlation between the gas content and the structure of the gravitational potential is observed Alard (2011). This analysis is reinforced by the results of Lelli et al. (2013) and Lelli et al. (2014) who find similar results with the additional finding that the structure of the potential is also related to the star formation activity. These observational results show that baryonic process related to stellar formation are responsible for the modification of the gravitational potential. However the detailed sequence of the events leading to these observational correlation is not clearly defined. A possibility is that most of the DM halo re-shaping occur at an early epoch when the star formation is very active, or that a number of particularly strong starburst has a major influence. However, the observational result from Kauffmann (2014) suggest that the total amount of energy released by the stellar formation is the real and fundamental parameter. It is important to note that the detailed sequence of the events do not really matter as long as the global process remain self similar.

Actually the dark matter core size r_{DM} is constructed by a dominant baryonic process P which has a typical scale length r_B , basically $P = P\left(\frac{r}{r_B}\right)$. The width at half maximum r_P of P reads, $r_P = P^{-1}\left(\frac{P(0)}{2}\right)r_B$. Thus $r_{DM} = kr_B$, with a constant of proportionality k depending on the specific functional form for P . Note that if we had estimated the typical

scale length of the process P not by taking the width at half maximum, but by taking the width at any other fractional value, it would change the value of k but we would still have, $r_{DM} \propto r_B$. Interestingly, Donato *et al.* (2004) found that the baryonic and dark matter scale length are nearly proportional. Similarly a correlation between the rotation curve and the baryonic distribution is also reported by Swaters *et al.* (2013). The strength of the baryonic influence on the dark matter kinematics must be compared to the gravitational force due to dark matter. If the baryonic force dominates we are in a pure flat core regime, while in the case where the dark matter force dominates we return to the NFW profile (Navarro, Frenk, & White, 1997). The intermediate regime when the dark matter force F_{DM} and baryonic force F_B are of the same order defines the typical size of the baryonic core induced regime. The force is proportional to the acceleration thus the dark matter core size r_{DM} corresponds to the following condition:

$$a_{DM}(r_{DM}) = a_B(r_{DM}) \tag{1}$$

Assuming a Burkert profile for the dark matter (Burkert (1995)), Gentile *et al* (2009) found that at a Burkert profile scale length r_0 the respective dark matter and baryonic acceleration are: $3.2_{-1.2}^{+1.8} 10^{-9} \text{cm s}^{-2}$ and $5.7_{-2.8}^{+3.8} 10^{-10} \text{cm s}^{-2}$. The radius corresponding to a half of the central value for the Burkert profile is $r_{DM} \simeq 0.55 r_0$. Assuming that most of the baryon mass is inside r_{DM} , the baryons in the range $r_{DM} < r < r_0$ behave like a point mass, the acceleration at r_0 must be re-normalized by the scale factor $\left[\frac{r_{DM}}{r_0}\right]^2$ to obtain the acceleration at r_{DM} . On the other hand the acceleration due to the Burkert acceleration decrease by about 13%. These corrections implies that $a_{DM}(r_{DM}) \simeq 2.8_{-1.0}^{+1.6} 10^{-9} \text{cm s}^{-2}$ and $a_B(r_{DM}) \simeq 1.9_{-0.9}^{+1.3} 10^{-9} \text{cm s}^{-2}$. These values of the acceleration are consistent with Eq. 1 within the errors bars. This result shows that the scale length of the dark matter halo core radius is consistent with the strength of the baryonic influence. The radial distance scale of dark matter is imposed by the baryons, which in itself is not sufficient to impose another similarity class to the dark matter halo. However as we shall see an equilibrium

condition for the gas also implies a constraint on the total force at the distance scale, which is only compatible with a specific similarity class.

2.1. Critical condition for optically thick gas.

We consider the effect of the baryonic feedback on a galaxy composed of stellar populations gas and dark matter. The momentum driven winds offer an efficient mechanism to drive winds over large distances. A potential problem in this model is that the gas and dust are ejected from the galaxy and sent to the intergalactic medium. However to have an effect on the DM halo there must be a cycle where matter is ejected and fall back on the galaxy. But contrary to conventional wisdom Oppenheimer & Davé (2008) show that a cycle occur in the momentum driven wind model, the ejected material is far more likely to fall back rather than stay in the inter galactic medium, with a typical fall back time of 1 Gyr. Note that the critical opacity (optically thick limit) is reached very quickly in a galaxy due to the production of dust by supernovae. Murray, Quataert & Thompson (2005) shows that the critical opacity is reached in only 10^6 years for a major starburst. As a consequence we will work in the optically thick limit where the equivalent starburst luminosity L_B of the stellar population is entirely absorbed by the gas. The mass distribution $M(r)$ is assumed to be spherically symmetric. Murray, Quataert, & Thompson (2005) proposed that such systems are prone to reach a critical luminosity $L_B = L_M$. If $L_B > L_M$ (which in general is expected) the acceleration of the gas layer is positive and the system loses mass which in turns decrease the star-burst activity. This mechanism operates until the star-burst luminosity reach the critical limit L_M . The luminosity L_M corresponds to an equilibrium between the momentum deposition of the radiation in the gas and the gravitational force applied to the gas.

2.1.1. *Gas distributed in a ring.*

Murray, Quataert, & Thompson (2005) studied this equilibrium for a gas component distributed in a shell. In this case the gas shell diameter is supposed to be close to the typical size of the galaxy r_B , which is proportional to the dark matter core size r_{DM} . Considering a total mass of gas M_G the equation corresponding to the equilibrium condition reads:

$$\frac{GM M_G}{r_B^2} = \frac{L_M}{c} \quad (2)$$

The starburst luminosity is associated with young stars, and the kinematics of these stars is not much different from the kinematics of the cold molecular gas, thus the mass loss affecting this population of stars will be proportional to the mass loss of the cold molecular gas. Since we expect that the rate of new stars will be also proportional to the cold molecular gas mass, the total number of stars in the starburst population will be proportional to the cold molecular gas mass. High quality observations by Tacconi et al. (2010), demonstrate that the fraction of cold molecular gas was much higher at the epoch of galaxy formation than what it is today. On average the fraction of molecular gas is at about 40 % when galaxies are forming, which is quite uncommon at the present time. The variability of the molecular gas fraction is also smaller at the epoch of galaxy formation, which justifies the approximation that the total gas mass and the cold molecular gas mass are proportional. The starburst population goes like the cold molecular gas and that the cold molecular gas mass is approximately proportional to the gas mass in forming galaxies. Thus we consider that the amount of stars in the starburst population will be approximately proportional to the total gas mass, which corresponds to the following relation:

$$L_M \propto M_G \quad (3)$$

By combining Eqs (2) and (3) we obtain the following equation:

$$\frac{GM}{r_B^2} = \text{Constant} \quad (4)$$

2.1.2. *General gas distribution.*

In the general case, assuming a density distribution ρ_G of the gas, the equilibrium at $r = r_B$ condition reads:

$$\int_0^{r_B} \rho_G(r)M(r)dr \propto \frac{L_M}{c} \quad (5)$$

Applying again Eq. 3 we obtain:

$$\int_0^{r_B} \rho_G(r)M(r)dr \propto M_G \quad (6)$$

In case of a stable equilibrium, the total force must be null at the point of equilibrium but also its first derivative. If we assume that an equilibrium is effectively realized at a typical baryonic scale r_B , we have:

$$\frac{GM}{r_B^2} = \text{Constant} \quad (7)$$

2.1.3. *Consequences of the baryonic critical condition for the self similar solution.*

Eq. (7) implies that the mass scales like the square of the radius of the distribution which is not consistent with the Bertschinger self similarity class. The nature of the baryonic scaling implies that $r_B \propto r_{DM}$, adopting $r_{DM} = \lambda r_B$, using Eq. (7) and defining a scale free acceleration, $a(r) = a_2 \left(\frac{r}{r_{DM}} \right)$, we have, $a(r_B) = \frac{GM}{r_B^2} = a_2 \left(\frac{1}{\lambda} \right) = \text{constant}$. Thus the acceleration is constant at a fixed point in re-scaled coordinates. The self similar regime associated with this constant acceleration corresponds to a specific scaling of the distance and velocity variables. The development of a new self similar regime induced by conditions developing near the center of the distribution remind us of the of the situation observed for the Binney conjecture (Binney (2004)) . In the two dimensional phase space the Binney conjecture states that for a large variety of initial conditions the system converges to a power law with an exponent equal to $-\frac{1}{2}$. It was demonstrated by Alard (2013) that the power law is induced by a singularity developing at the center of the system. Note that

since the scale length of the dark matter self similar solution is time dependent, the scale length of the baryonic distribution must be also time dependent. However we consider a near equilibrium situation where the temporal variation of the baryonic scale radius is small compared to the system typical time scale, thus the baryonic and dark matter scale length need only to be asymptotically identical. It is expected that the variation of the baryonic scale length is due to the slow accretion of new baryonic material.

2.2. Self similar solutions of the Vlasov-Poisson system.

Before we relate the baryonic scaling obtained in the previous section to a given similarity, let first remind some of the results obtained in Alard (2013) on the self similar solutions of the Vlasov-Poisson system. Given a phase space density $f(\mathbf{x}, \mathbf{v}, t)$ the general solution in six dimensional phase space reads:

$$\begin{cases} f(\mathbf{x}, \mathbf{v}, t) = t^{\alpha_0} g\left(\frac{r}{t^{\alpha_1}}, \frac{\mathbf{v}}{t^{\alpha_2}}\right) \\ \alpha_0 = -2 - 3\alpha_2 \quad ; \quad \alpha_1 = 1 + \alpha_2 \end{cases} \quad (8)$$

Eq. (8) implies that the density ρ has the following time scaling:

$$\rho(r) = \int g(r, \mathbf{v}, t) d^3v = t^{-2} \rho_2\left(\frac{r}{t^{\alpha_1}}\right)$$

Consequently the time scaling of the acceleration reads:

$$a(r) \propto \frac{M}{r^2} = \frac{1}{r^2} \int \rho(r) r^2 dr = t^{-2+\alpha_1} a_2\left(\frac{r}{t^{\alpha_1}}\right) \quad (9)$$

The self similar growth of a given dark matter halo with the constraint from Eq. (8) implies that the acceleration at a given re-scaled coordinate remains constant (see Sec. 2.1.2).

Thus Eq. 9 should depend only on the re-scaled coordinate and not on time. Considering the growth of an individual dark matter halo with typical scale $r_{DM}(t)$, Eq. (8) implies

that the acceleration at $r_{DM}(t)$ is constant. Assuming a slow adiabatic process the time dependence of the re-scaling factor in Eq. (9) can be linearized. The same linearization can be applied to $r_{DM}(t)$ which implies that the two expressions become compatible, and that $r_{DM}(t)$ can be identified to the scaling factor t^{α_1} . Considering this identification, Eq. (9) coupled with Eq. (7) implies that $\alpha_1 = 2$, and $\alpha_2 = 1$. Thus the new similarity class corresponds to $\alpha_2 = 1$, this must be compared to the initial Bertschinger similarity class, where the similarity was imposed by the nature of the cosmological infall and corresponds to, $\alpha_2 = -\frac{1}{9}$.

2.2.1. Correspondence between time and distance scales.

The halo velocity and distance scales are related to a free parameter t_0 in the definition of time for the self similar solution. Basically if $f(\mathbf{x}, \mathbf{v}, t)$ is a solution then $f(\mathbf{x}, \mathbf{v}, \frac{t}{t_0})$ is also a solution. By introducing t_0 the scaling of r and v are transformed to respectively, $\left(\frac{t}{t_0}\right)^{\alpha_1}$ and $\left(\frac{t}{t_0}\right)^{\alpha_2}$. The corresponding re-scalings of r and v are $x_0 = t_0^{-\alpha_1}$ and $v_0 = t_0^{-\alpha_2}$. For the final stage of the evolution of an individual halo a_{DM} does not depend on time, which also implies that a_{DM} does not depend on t_0 , and thus does not depend on x_0 or v_0 . These results illustrates the correspondence between time and scale independence. Equation (7) implies that the total acceleration at r_B is scale free and since a_{DM} is scale free at all positions, the baryonic acceleration at r_B , $a_{0B} = a_B(r_B)$ is scale free or time independent. The baryonic acceleration at larger distances, out of the baryonic distribution is properly approximated with the acceleration due to a single massive point, thus,

$$a_B \simeq a_{0B} \left(\frac{r_B}{r}\right)^2 \quad r > r_B \quad \text{with} \quad a_{0B} = a_B(r_B) \quad (10)$$

Eq. (10) indicates that at larger distances a_B is only a function of scale free variables and as a consequence is scale free. Since a_{DM} is also scale free the total acceleration at larger distances ($r > r_B$) is scale free. The fact that the both the baryonic and dark matter

accelerations are independent of scale is supported by the observations. Gentile (2009) found that at a specific scale length r_0 ($r_0 \simeq 1.8 r_{DM}$), the baryonic and dark matter acceleration are constant.

3. Connection to MOND.

Milgrom (1983), and Bekenstein & Milgrom (1984), developed an empirical modification of Newtonian dynamics in order to reproduce the rotation curves of galaxies without the need of including a dark unseen component. The remarkable success of this approach in reproducing the data (see for instance Milgrom & Sanders (2007), Milgrom (2001), Milgrom (1995)) is particularly compelling since the modelisation is based on parameters reconstructed directly from the distribution of visible matter. Mond assumes that a transition from the Newtonian regime occurs at an acceleration $a_0 \simeq 10^{-10} \text{cm s}^{-2}$ and that below this acceleration we observe an evolution to the deep MOND regime which represents the very low acceleration limit. Between the Newtonian and deep MOND regime an empirical interpolation function is assumed. There are various models for the interpolation function with the obvious consequence that this intermediate regime is not a very well defined feature of MOND. The essential feature are clearly the acceleration scale at which the transition occurs and the properties of the deep MOND regime at very low accelerations. These two features derived from MOND are clearly related to universal properties of galaxies and have to be reproduced by any theory aiming to represent the mass distribution in galaxies. As we will see the baryonic induced self similar model is consistent with these MOND features. Let's now review MOND general properties and confront them with the self similar model. For spherically symmetric systems the new equation reads:

$$\mu\left(\frac{a}{a_0}\right) a = a_B \tag{11}$$

3.1. Scale free behavior of MOND.

Milgrom (1986) already noticed that a similarity relation existed in the MOND approach and that Eq. 11 can be written in a dimensionless form (see Milgrom 1986, Eq. 5). At larger distances $r > r_B$ it is straightforward to re-write Eq 11 using Eq. 10:

$$\mu\left(\frac{a}{a_0}\right)a = a_{0B}\left(\frac{r_B}{r}\right)^2 \quad (12)$$

The constant a_{0B} is independent of scale thus the acceleration in Eq. 12 is only of a function of scale free variables. In the self similar model the dark matter acceleration is scale free, the baryonic acceleration (Eq. 10) is scale free at larger distances, thus the total acceleration is scale free at larger distances ($r > r_B$), which is consistent with Eq. (12).

3.2. Rotation curves in MOND and the self similar model.

A general feature of the MOND phenomenology is that at larger distances ($r \gg r_B$, and $a \ll a_0$), the Newtonian force field is a point mass field which implies that the relation between the velocity at large distances, v_M and the baryon mass M_B is:

$$v_M^4 = a_0 G M_B \quad (13)$$

The velocity at $r \gg r_B$ in the self similar model corresponds to the maximum of the velocity curve v_M , which for a typical dominant dark matter profile, occurs at larger distances (see Fig. 1 for an illustration corresponding to a Burkert profile). We define the position the position of the maximum of the self similar velocity curve r_M , with, $r_M = \eta r_{DM}$, then

$\frac{v_M^2}{r_M} = a_M$, is scale free, and we obtain:

$$v_M^4 = \eta^2 \frac{a_M^2}{a_B(r_{DM})} G M_B \quad (14)$$

An identification between Eq. 13 and Eq. 14 indicates that $a_0 = a_B(r_{DM}) \left(\frac{a_M}{a_B(r_{DM})}\right)^2 \eta^2$.

We will adopt $a_B(r_{DM}) \simeq a_{DM}(r_{DM}) \simeq 2 \cdot 10^{-9} \text{ cm s}^{-2}$ (see Sec. 2). Note that

$\frac{a_M}{a_B(r_{DM})} = \frac{a_2(\eta)}{a_2(1)}$ is scale free and thus a constant, since the acceleration is scale free at larger distances. Assuming that an estimation of the constants can be obtained by modeling the mass distribution with a Burkert profile, $\frac{a_M}{a_{DM}(r_{DM})} \simeq \frac{1}{2}$ and $\eta \simeq 6$, we obtain, $a_0 \simeq 1.8 \cdot 10^{-8} \text{ cm s}^{-2}$. Milgrom (2001) estimated that a_0 is of the order of $10^{-8} \text{ cm s}^{-2}$ which is consistent, and shows that the MOND and the self similar model have the same expectation at large distances. An additional point is that the self similar model predicts that at a characteristic scale r_{DM} the acceleration due to the baryons is of the order of the acceleration due to dark matter. The scale free behavior of the acceleration implies effectively that at the distance scale r_{DM} the acceleration is constant. The region $r \simeq r_{DM}$ corresponds to the MOND intermediate regime, where the function $\mu(x)$ is between the Newtonian regime $\mu = 1$ and the deep MOND regime, $\mu = x$. The fact that the transition between the baryon dominated regime and the dark matter regime occurs at a fixed acceleration in the self similar model is a clear connection to MOND. To compare the acceleration \bar{a} at which the transition occurs in the two approach we have to consider the equivalent of the situation where $a_{DM} = a_B$ in the MOND approach. Considering Eq. 11 this will corresponds to $\bar{a} = 2a_B$, which in turn implies,

$$\mu\left(\frac{\bar{a}}{a_0}\right) = \frac{1}{2} \quad (15)$$

Begeman et al. (1991) showed that a sample of high quality rotation curves of galaxies could be fitted using $\mu = \frac{x}{\sqrt{1+x^2}}$ and $a_0 = 1.2 \pm 0.27 \cdot 10^{-8} \text{ cm s}^{-2}$. Using these results the solution of Eq. 15 is $\bar{a} \simeq 0.69 \pm 0.16 \cdot 10^{-8} \text{ cm s}^{-2}$. The results of Sec. 2 implies that in the self similar model $\bar{a} = a_{DM}(r_{DM}) + a_B(r_{DM}) \simeq 0.47_{-0.13}^{+0.21} \cdot 10^{-8} \text{ cm s}^{-2}$ which is consistent with the MOND value for \bar{a} considering the error bars. We compared the large distance low acceleration and intermediate regime between MOND and the self similar model. In the remaining domain ($a \gg a_0$) the dynamic is Newtonian and since in galaxies this regime also occurs at shorter distances from the center ($r \ll r_{DM}$) the baryons dominates and will thus satisfies the Newtonian limit of MOND (Eq. 11). As a

consequence the asymptotic limits in the MOND and self similar approach are the same, the difference is only a matter of interpolation between the low acceleration and Newtonian limits. In MOND the interpolation function itself is not defined in the theory and is free to vary within some limited constraints. However there is a significant difference between the self similar model and MOND, the equilibrium equation (7) applies to a galaxy, but some fundamental mechanisms are missing to apply it to clusters of galaxies. Despite the fact that core formation via a feedback due to AGN has been found to operate in clusters of galaxies (Martizzi, Teyssier, & Moore, (2013)), the nature of the process does not include a regulation mechanism that would lead to an equilibrium condition like Eq. (7). In galaxies the regulation operates by interaction between star formation and the loss of gas. If star formation is too high the wind are higher than the critical limit, which implies that gas is removed and as a result slow down star formation (Murray, Quataert & Thompson (2005)). Such regulation mechanism does not exist with the AGN feedback model of Martizzi, Teyssier, & Moore, (2013). As a consequence this self similar model and its associated phenomenology should not be present in cluster of galaxies, which is a clear difference with MOND. This break of the phenomenology is in good agreement with the observations as illustrated with the case of the Bullet cluster (Clowe et al. (2006), and Clowe et al. (2004)).

4. Density and pseudo-phase space density of dark matter halos.

It was demonstrated in Alard (2013) that the pseudo-phase space density of self-similar solutions of the Vlasov-Poisson system has a power law behavior. When this result is coupled with the Jeans equation an equation for the density can be obtained (see Dehnen et al. (2005) for a discussion in the case of the Bertschinger similarity class). This section will now discuss the solution for the density in the case of the baryonic induced

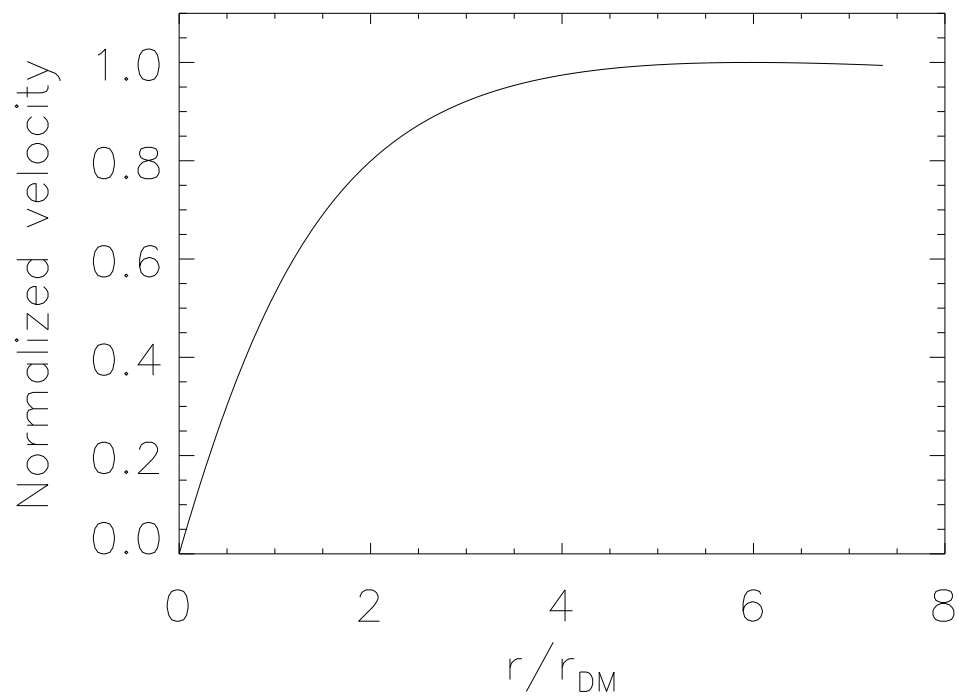


Fig. 1.— The rotation velocity associated with a Burkert profile. The maximum of the velocity curve was normalized to unity. The radial coordinates is scaled using the the Burkert profile scale length r_{DM} .

similarity class. It is clear that changing the similarity class has a major influence on the solution for the density, and that the work already conducted for the similarity class $\alpha_2 = -\frac{1}{9}$ needs to be re-conducted for the new similarity class $\alpha_2 = 1$. We will assume a spherically symmetric system, thus the spatial coordinates will be reduced to the radial distance modulus r . The Jeans equation reads:

$$\frac{1}{\rho} \frac{d}{dr} (\rho \sigma^2) + \frac{2\beta \sigma^2}{r} + \frac{G}{r^2} \int_0^r \rho u^2 du = 0 \quad (16)$$

The pseudo-phase space density $\frac{\rho}{\sigma^3}$ is a power law with predictable exponent for the self similar solutions of the Vlasov-Poisson system (Alard 2013). The exponent is a function of the self similar solution constant α_2 , $\frac{\rho}{\sigma^3} \propto \left(\frac{r}{r_0}\right)^\gamma$, and $\gamma = -\frac{2+3\alpha_2}{1+\alpha_2}$. In the regime of the imposed baryonic self similarity, $\alpha_2 = 1$, thus $\gamma = -\frac{5}{2}$. It is useful to define the density and anisotropy parameter as a function of the re-scaled variable, $u = \frac{r}{r_0}$:

$$\rho(r) = \rho_0 \rho_s(u) \quad ; \quad \beta(r) = \beta_s(u) \quad ; \quad \sigma(r) = \sigma_0 \sigma_s(u) \quad ; \quad M(r) = \rho_0 r_0^3 M_s(u) \quad (17)$$

The Jeans equation in these variables reads:

$$5u \frac{d^2 M_s}{du^2} - 5 \frac{d}{du} M_s + 6\beta \frac{dM_s}{du} + 3q_0 \left[\frac{dM_s}{du} \right]^{\frac{4}{3}} = 0 \quad (18)$$

By applying a derivative to Eq. 18 an equation for the density ρ is obtained.

$$\rho_s \left(15u \frac{d^2 \rho_s}{du^2} + \rho_s \left(18 \frac{d\beta_s}{du} + \frac{1}{u} (48\beta + 40) \right) + \frac{d\rho_s}{du} (65 + 12\beta) \right) - 5u \frac{d\rho_s}{du}^2 + q_0 \rho_s^{\frac{7}{3}} u^{-\frac{2}{3}} = 0 \quad (19)$$

With the following definition for the parameter q_0 :

$$q_0 = \frac{9G\rho_0 r_0^2}{\sigma_0^2}$$

Assuming that the halo is virialized at radius r_0 , we obtain an estimation of the parameter q_0 .

$$\int GM\rho r dr \simeq \int \rho\sigma^2 r^2 dr$$

With:

$$\frac{\rho}{\sigma^3} = \frac{\rho_0}{\sigma_0^3} u^{\frac{5}{2}}$$

The former equation reads:

$$q_0 \int GM_s \rho_s u du = \int \rho_s^{\frac{5}{3}} u^{\frac{11}{3}} du \quad (20)$$

Equation 20 provides a direct estimation of q_0 .

4.1. General solution and asymptotic properties.

There are two types of asymptotic regimes to consider, a power law or a constant core.

4.1.1. Power law asymptotic behavior.

The power law solution for a similar equation was already discussed extensively by Dehnen & McLaughlin (2005). The asymptotic behavior at origin is related to the dominant behavior of the left term in Eq. 16, which implies an asymptotic solution of the type $\rho\sigma^2 \equiv \text{constant}$. As a consequence, with $\rho \propto r^\alpha$ and $\frac{\rho}{\sigma^3} \propto r^\gamma$ the corresponding asymptotic behavior is $\alpha = \frac{2}{5}\gamma$. For the Bertschinger solution, $\alpha_2 = -\frac{1}{9}$, $\gamma = -\frac{15}{8}$, and $\alpha = -\frac{3}{4}$ which corresponds to the results obtained by Dehnen & McLaughlin (2005). For the solution discussed in this paper $\gamma = -\frac{5}{2}$, and $\alpha = -1$. Note that $\alpha = -1$ is the limit for the dominance of the left term in Eq. 16, and that as a consequence we have a full solution of the equation, not just for the dominant term.

4.1.2. *Constant core asymptotic behavior.*

The observations favor models with constant density core, like cored iso-thermal models Spano et al. (2008) or the Burkert profile (Burkert (1995)). In such case the general solution of Eq's 18 and 19 writes:

$$\left\{ \begin{array}{l} \rho_s = \sum_{n=0}^{\infty} a_n u^{\frac{n}{3}} \\ \beta_s = \sum_{n=0}^{\infty} b_n u^{\frac{n}{3}} \end{array} \right. \quad (21)$$

It is interesting to write explicitly the first terms of the solution series expansion:

$$b_0 = -\frac{5}{6} \quad b_1 = \frac{\frac{5}{3}a_1 + q_0 a_0^{\frac{4}{3}}}{6a_0} \quad b_2 = \frac{(100a_2 a_0 + 7q_0 a_0^{\frac{4}{3}} a_1 - 50a_1^2)}{180a_0^2} \quad (22)$$

A general property of the solutions presented in Eq. 22 is that the zeroth order term in the expansion of β is constant. Another point is that in general the next terms in the expansion are of low order in u , unless these terms are equal to zero, the asymptotic behavior of β at origin will not correspond to a local minimum of the function. An approximate estimation of the functional β is obtained by assuming a simple empirical model known for its good consistency with the observations, like the cored isothermal model:

$$\rho_s \propto \frac{1}{(1 + u^2)^{\frac{3}{2}}}$$

Or the Burkert profile:

$$\rho_s \propto \frac{1}{(1 + u)(1 + u^2)}$$

The functional β is directly estimated by introducing these models of the density in Eq. (18), the results are presented in Fig. 2. The variable q_0 is estimated using Eq. (20), we find $q_0 \simeq 3.2$ for the cored isothermal density and $q_0 \simeq 3.4$ for the Burkert profile. Both profiles converge at $\beta = -\frac{5}{6}$ at the origin and cross the zero line near $u = 1$, at larger distances increase slowly and converge to radial orbits at infinity, which is consistent with

the cosmological infall. Although these profiles allows us to reproduce the general features of β , a generic problem is that in both case the minimum of β is not situated at origin. Another way to consider the problem would be to assume a generic behavior for β and estimate ρ . The fixed properties of β are the value at the origin and the crossing of the zero line at $u = 1$. If we add that the minimum of β must be located at the origin, it is straightforward to infer a parabolic model for β .

$$\beta = \frac{5}{6}(u^2 - 1) , \quad 0 < u < 1 \quad (23)$$

By introducing Eq. (23) in Eq. (19) we obtain an equation for ρ . The solution of this differential equation is obtained numerically using a Runge Kutta method. Finding the solution requires a value of q_0 , but since q_0 is unknown at the initial step, a first guess is assumed for q_0 , a solution is found and q_0 is estimated. This process is iterated until the guess for q_0 and the value estimated from the numerical solution are the same. We start from $q_0 = 3$ which corresponds approximately to the values obtained for the cored isothermal and Burkert profiles. Starting from this initial value the iteration process converges to a value of $q_0 = 5.59$. The numerical solution for ρ corresponding to the simple asymptotic model of β at origin described in Eq. (23) is closely approximated with a Einasto profile (Einasto (1972)):

$$\rho(r) \propto \exp\left(e_0 r^{\frac{1}{n}}\right) \quad (24)$$

Note that the nature of the expansion in Eq. (21) implies that if the solution is consistent with an Einasto profile, then we have necessarily $n = 3$.

5. Synthesis and conclusion.

The main concept presented in this article is that the initial dark matter self similarity is affected by the baryon feedback and replaced with a baryonic induced self similarity. It

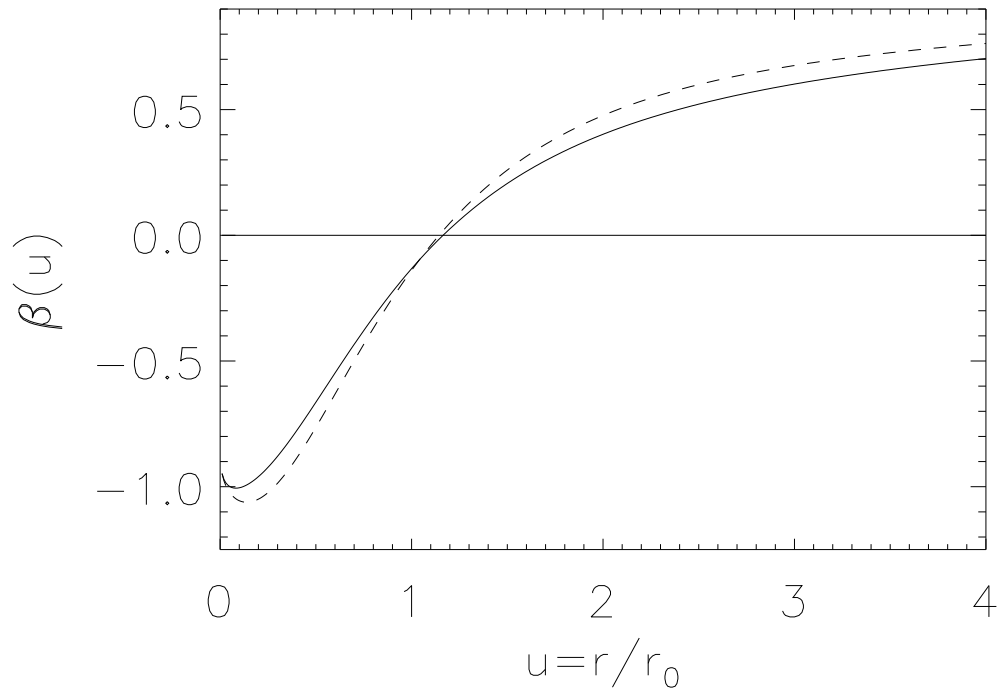


Fig. 2.— The anisotropy parameter β for the cored isothermal profile (dashed line) and for the Burkert profile.

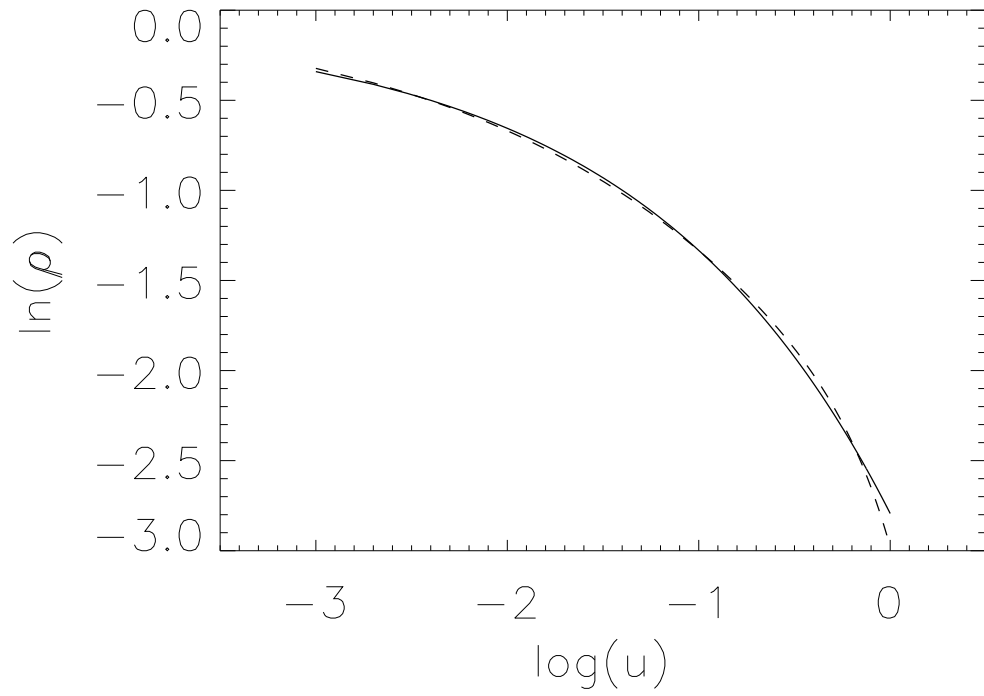


Fig. 3.— The dotted line represents the density obtained by solving Eq. 19 for a functional β given by Eq. 23. The continuous line is the adjustment of an Einasto profile ($n = 3$) to the numerical solution.

was demonstrated in Sec. (2.1) that the baryonic feedback impose two conditions on the dark matter distribution. These baryonic constraints are not compatible with the initial similarity class. Provided that the solution remains self similar, the conditions from Sec. (2.1) imply the emergence of a new similarity class for the dark matter halo. An important point is that this model relies on the assumption that an equilibrium is obtained between the wind pressure and the gravity of the system, leading to a baryonic induced similarity of the DM halo. However to reach this equilibrium the equivalent luminosity L must be greater than some critical luminosity L_M (Murray, Quataert & Thompson (2005)). Obviously if the star formation in the galaxy is not sufficient to reach this critical luminosity, no universal acceleration would exists and the associated self similarity class would not be present. In this case it is not even clear that any self similar properties would emerge from the baryonic feedback. But we must keep in mind that violating the equilibrium condition would definitely go against the observations, and the universal accelerations for the galaxies observed by Gentile et al. (2009). This would also again go against the general MOND conjecture Milgrom (1983), Milgrom (1986), Milgrom (1995), Milgrom (2001). Another crucial assumption is the proportionality between the luminosity and the mass of gas (see 2.1, Eq. 3). An open possibility is that the scale factor between mass and luminosity in Eq. 3 depends on galaxy type. As a result we would still have a baryonic induced self similarity for each galaxy, but the similarity parameter (the constant in Eq. 4), which is an acceleration would depend on galaxy type. Interestingly Del Popolo et al. (2013) found that the acceleration constant estimated by Gentile et al. (2009) is correlated to the mass of the galaxy, which would support the fact that the scaling in Eq. 3 depends on galaxy type. A direct consequence of this finding is also to support the fact that the nearly universal relations observed for galaxies are due to internal physics within the galaxies, a category to which the baryonic feedback obviously belongs. A final and crucial assumption is that the effect of the baryonic feedback is sufficient to induce a new class of similarity in the

DM halo. It is reasonable to consider that the baryonic feedback is sufficient to alter the shape of the DM core and that this process has self similar properties. But does this mean that this baryonic self similarity is transmitted to the whole DM halo ? It is clear that at least self similarity should be transmitted in some domain with boundaries scaling like the typical of the scale of the baryonic distribution. However, does this mean that the baryonic self similarity will be transmitted to the very central region, does self similarity break at some small fraction of the baryonic scale ? We should also expect that self similarity breaks at some distance in the outer regions. At the moment the answer to these questions is not clear, but hopefully some new insight should come from the detailed exploration of this type of model using numerical simulations. A possible observational test of self similarity is provided in Sec. 4, with the prediction of an Einasto profile with index $n = 3$. However the reconstruction of the parameters of an Einasto profile is especially difficult due to the intrinsic difficulty of subtracting the baryon contribution in the inner region (Chemin, de Blok, & Mamon (2011)). One important property of this new self similar solution is that the acceleration generated by the dark matter halo is scale free. When combined with the properties of the baryonic feedback, the scale free acceleration of the dark matter implies that the baryon acceleration at one scale radius r_{DM} is independent on r_{DM} . This self similar model put a number of observational facts on galaxies in a coherent framework. First, the universality of the baryon and dark matter accelerations observed at a scale radius of the dark matter distribution for a large number of galaxies (Gentile *et al* 2009), and second this self similar model is related to the MOND phenomenology of galaxies (Milgrom 1983, and Bekenstein & Milgrom 1984). An additional point is that the density corresponding to this self similar model is expected to form a flat cored distribution in the central region, and a large variety of profiles has been proposed to fit the observations, cored isothermal, Burkert, or Einasto profiles. Among these possibilities, the Einasto profile has the best compatibility near the origin with the expectation from the self similar, baryonic

induced model. In these results it is of particular interest to point out that the in self similar model CDM and MOND become consistent with each other . The general features observed in the rotation curves of galaxies are properly described in the MOND framework, but we see that it can be as well represented by dark matter self similar solution.

The incompatibility of the MOND phenomenology and of the observations in general is a serious problem for the cold dark matter model (See for instance Kroupa et al. (2012) for a review). Thus the result that this new cold dark matter model based on self similarity is consistent with the observed phenomenology is definitely a change in the CDM paradigm. A major difference between the MOND approach and the self similar CDM model is that the self similar model does not apply to clusters of galaxies, since the equilibrium condition (Eq. 7) does not apply to a cluster. The discrepancies between the MOND phenomenology and the observations of the Bullet cluster are thus predicted by the self similar model.

The author would like to thank J.P. Beaulieu and S. Colombi for comments, and the referee for interesting suggestions. This work has been funded in part by ANR grant ANR-13-MONU-0003.

REFERENCES

- Alard, C., 2013, MNRAS, 428, 340
- Alard, C., 2011, ApJ Letters, 728, 47
- Benson, A., 2010, Physics Reports, 495, issue 2-3, 33
- Binney J., 2004, MNRAS, 350, 939
- Bekenstein, J., Milgrom, M., 1984, ApJ, 286, 7
- Bertschinger, E., 1985, ApJS, 58, 39
- Burkert, 1995, ApJL, A., 447, 25
- Butsky, I., Maccio, A. V., 2014, AAS, 223, 246.46
- Chemin, L., de Blok, W., Mamon, G., 2011, AJ, 142, 109
- Clowe, D., Bradac, M., Gonzalez, A., Markevitch, M., Randall, S., Jones, C., Zaritsky, D.,
2006, ApJ, 648, 109
- Clowe, D., Gonzalez, A., Markevitch, M., 2004, ApJ, 604, 596
- de Blok, W.J.G., Walter, F., Brinks, E., Trachternach, C., Oh, S.-H. and Kennicutt Jr,
R.C., 2008, Astron. J., 136, 26482719
- Davé, R., Finlator, K., Oppenheimer, B. D., 2007, EAS Publications Series, 24, 183
- Dehnen, W., McLaughlin, D., 2005, MNRAS, 363, 1057
- Del Popolo, A., Cardone, V., Belvedere, G., 2013, MNRAS, 429, 1080
- Donato, F., Gentile, G., Salucci, P., Frigerio M., Wilkinson, M., 2009, MNRAS, 397, 1169

- Di Cintio et al., 2013, MNRAS, 431, 1220
- Donato, F., Gentile, G., Salucci, P., 2004, MNRAS, 353, 17
- Einasto J., Einasto L., 1972, Tartu Astrofüüsika Observatoorium Teated, 36,3
- Gentile, G., Famaey, B. and de Blok, W.J.G., A&A, 2011, 527, 76
- Gentile, G., Famaey, B., Zhao, H., Salucci, P., 2009, Nature, 461, 627
- Gnedin, O. Y., Zhao, H., 2002, MNRAS, 333, 299
- Governato, F., 2012 et al., MNRAS 422, 1231
- Kauffmann, G., 2014, arXiv 1401.8091
- Kroupa, P., Pawlowski, M., Milgrom, M., IJMPD, 2012, Volume 21, Issue 14, id. 1230003
- Lapi, A., Cavaliere, A., 2011, ApJ, 743, 127
- Lelli, F., Fraternali, F., Verheijen, M., 2014, A&A Letters, 563, 27
- Lelli, F., Verheijen, M., Fraternali, F., Sancisi,
- Lelli, F., Verheijen, M., Fraternali, F., Sancisi, R., AAS, 22110702L
- Ludlow, A., Navarro, J., Springel, V., Vogelsberger, M., Wang, J., White, S., Jenkins, A.,
Frenk, C., 2010 MNRAS, 406, 137
- Martizzi, D., Teyssier, R., Moore, B., 2013, MNRAS, 432, 1947
- McQuinn et al., 2010, ApJ, 724, 49 R., AAS, 22110702L
- Ludlow, A., Navarro, J., Springel, V., Vogelsberger, M., Wang, J., White, S., Jenkins, A.,
Frenk, C., 2010 MNRAS, 406, 137

- Martizzi, D., Teyssier, R., Moore, B., 2013, MNRAS, 432, 1947
- McQuinn et al., 2010, ApJ, 724, 49
- Milgrom, M., Sanders, R., 2007, ApJL, 658, 17
- Milgrom, M., 2001, AcPPB, 32, 3613
- Milgrom, M., 1995, ApJ, 455, 439
- Milgrom, M., 1986, ApJ, 302, 617
- Milgrom, M., 1983, ApJ, 270, 384
- Murray, N., Quataert, E., Thompson, T., 2005, ApJ, 618, 569
- Navarro, J., Ludlow, A., Springel, V., Wang, J., Vogelsberger, M., White, S., Jenkins, A.,
Frenk, C., Helmi, A., 2010, MNRAS, 402, 21
- Navarro, J., Frenk, C., White, S., 1997, ApJ, 490, 493
- Navarro, J. F., Eke, V. R., Frenk, C. S., 1996, MNRAS, 283, L72
- Ogiya, G.; Mori, M., 2012, ASPC, 458, 385O
- Oh, S., de Blok, W. J. G., Brinks, E., Walter, F., Kennicutt, R. C., 2011, AJ, 141, 193O (a)
- Oh, S., Brook, C., Governato, F., Brinks, E., Mayer, L., de Blok, W. J.G., Brooks, A.,
Walter, F., 2011, AJ, 142, 24O (b)
- Oppenheimer, B., Davé, R., 2008, 387, 577
- Oppenheimer, B., Davé, R., 2006, MNRAS, 373, 1265
- Persic, M., Salucci, P., Stel, F., 1996, MNRAS, 281, 27

- Pontzen, A., Governato, F., 2014, *Nature*, 506, Issue 7487, 171
- Pontzen, A., Governato, F., 2013, *MNRAS*, 430, 121
- Pontzen, A., Governato, F., 2012, *MNRAS* 421, 3464
- Ragone-Figueroa, C., Granato, G. L., Abadi, M. G., 2012, *MNRAS*, 3092
- Read, J., Gilmore, G., 2005, *MNRAS*, 356, 107
- Salucci, P. Lapi, A. Tonini, C. Gentile, G. Yegorova, I. Klein, U., 2007, *MNRAS*, 378, 41
- Salucci P., Persic M., 1997, *ASPC*, 117, 1
- Spano, M., Marcelin, M., Amram, P., Carignan, C., Epinat, B., Hernandez, O., 2008, *MNRAS*, 383, 297
- Subramanian, K., 2000, *ApJ*, 538, 517
- Swaters, R. A., Sancisi, R., van der Hulst, J. M., van Albada, T. S., 2012, *MNRAS*, 425, 2299
- Tacconi et al., 2010, *Nature*, 463, 781
- Taylor, J.E., Navarro, J., F., 2001, *ApJ*, 563, 483
- Teyssier, R., Pontzen, A., Dubois, Y., Read, J. 2013, *MNRAS*, 429, 3068
- Walter, F., Brinks, E., de Blok, W.J.G., Bigiel, F., Kennicutt Jr, R.C., Thornley, M.D. and Leroy, A., 2008, *Astron. J.*, 136, 25632647